EJN EUROPEAN JOURNAL OF NEUROSCIENCE FENS Federation of European Neuroscience Societies

European Journal of Neuroscience, Vol. 40, pp. 2987–2997, 2014 doi:10.1111/ejn.12663

COGNITIVE NEUROSCIENCE

Dissociation of part-based and integrated neural responses to faces by means of electroencephalographic frequency tagging

Adriano Boremanse,[1] Anthony M. Norcia[2] and Bruno Rossion[1]
[1]Psychological Sciences Research Institute and Institute of Neuroscience, Université catholique de Louvain, 10 Place du Cardinal Mercier, Louvain la Neuve 1348, Belgium
[2]Department of Psychology, Stanford University, Palo Alto, CA, USA

Keywords: face perception, frequency tagging, human, intermodulation, repetition suppression, steady-state visual evoked potential

Abstract

In order to isolate the repetition suppression effects for each part of a whole-face stimulus, the left and right halves of face stimuli were flickered at different frequency rates (5.88 or 7.14 Hz), changing or not changing identity at every stimulation cycle. The human electrophysiological (electroencephalographic) responses to each face half increased in amplitude when different rather than repeated face half identities were presented at every stimulation cycle. Contrary to the repetition suppression effects for whole faces, which are usually found over the right occipito-temporal cortex, these part-based repetition suppression effects were found on all posterior electrode sites and were unchanged when the two face halves were manipulated by separation, lateral misalignment, or inversion. In contrast, intermodulation components (e.g. 7.14–5.88 = 1.26 Hz) were found mainly over the right occipito-temporal cortex and were significantly reduced following the aforementioned manipulations. In addition, the intermodulation components decreased substantially for face halves belonging to different identities, which form a less coherent face than when they belong to the same face identity. These observations provide objective evidence for dissociation between part-based and integrated (i.e. holistic/configural) responses to faces in the human brain, suggesting that only responses to integrated face parts reflect high-level, possibly face-specific, representations.

Introduction

The human brain has developed efficient mechanisms to recognize visual objects (Logothetis & Sheinberg, 1996; Thorpe *et al.*, 1996; DiCarlo & Cox, 2007). Object recognition requires the combination of different parts into a whole object (visual integration), and the differentiation of the object and its parts from other objects (visual discrimination). These issues are particularly important for the human face, as it is a complex stimulus made of multiple parts that need to be integrated into a unified percept (visual integration) and as different faces need to be discriminated from one another for adequate social interactions (individual face discrimination).

It is thought that the human brain discriminates faces by means of both part-based and integrated, i.e. holistic/configural, representations (Young *et al.*, 1987; Tanaka & Farah, 1993; Maurer *et al.*, 2002; Rossion, 2013). However, the respective contribution and nature of part-based and holistic/configural face representations are difficult to understand because conventional approaches do not allow separating (i) the neural responses arising from the perception of each of the facial parts presented simultaneously and (ii) these part-based responses from the response to the integrated stimulus that they form.

According to recent evidence, electroencephalographic (EEG) frequency tagging provides a unique way to tackle the problem of both visual discrimination and integration of facial parts in the human brain. Specifically, different face stimuli presented at a fixed rate elicit an electrical brain response at exactly that fundamental frequency rate, a steady-state visual evoked potential (SSVEP) (Regan, 1966) that is much larger over the right occipito-temporal cortex than when exactly the same face is repeated (Rossion & Boremanse, 2011; see, for a review Rossion, 2014). This repetition suppression effect is similar to the reduced neuronal response to repeated faces in the monkey inferior temporal cortex (Miller *et al.*, 1991; Ringo, 1996), as well as in the human ventral occipito-temporal cortex in neuroimaging (Grill-Spector *et al.*, 2006). It provides an objective (i.e. locked at an experimentally-defined frequency) signature of individual face discrimination. Moreover, there is recent evidence that tagging each half of a face with different frequency rates of stimulation (e.g. $f1$ = 5.88 Hz and $f2$ = 7.14 Hz; Fig. 1) provides an objective signature of integration [nonlinear intermodulation (IM)

Correspondence: Bruno Rossion, as above.
E-mail: bruno.rossion@uclouvain.be

Received 19 November 2013, revised 23 May 2014, accepted 30 May 2014

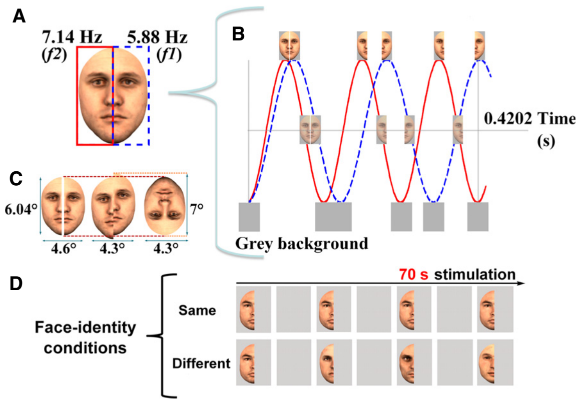

FIG. 1. Schematic illustration of the stimulation. (A and B) The left and right face halves are contrast modulated at different frequencies. Here the left part (thick red line) flickers at 5.88 Hz and the right part (dashed blue line) at 7.14 Hz. Note that the same facial identity is presented here (condition 'Same'). (C) The three control conditions of the study: 'Gap', 'Misaligned' and 'Inverted' faces. (D) Schematic illustration of the stimulation under the two face identity presentations – same identity (above) and different identities (below) depicted for the left face half only for clarity purposes. The four conditions were crossed with the two face identity presentations, yielding a total of eight different conditions.

responses] (e.g. 7.14–5.88 = 1.26 Hz). These IM responses are produced by neuronal populations that integrate the two face parts nonlinearly. Hence, they decrease substantially when the structural integrity of the face is broken, for instance when the two halves are not aligned with each other (Boremanse *et al.*, 2013).

Here, we built upon these sources of evidence to compare part-based (fundamental frequencies) and integrated (IM frequencies) EEG responses when the two halves of a face stimulus change identity independently, at specific frequency rates. In doing so, we tested (i) whether there are neural repetition suppression effects that can be unambiguously attributed to only the parts of a face, (ii) the influence of the structural integrity of the face on these putative part-based repetition suppression effects, and (iii) how these part-based effects relate to the nonlinear integration processes represented by IM responses.

Materials and methods

Participants

Eleven healthy adults (all right-handed; two males; age 19–28 years, median age 23 years) whose visual acuity was either reported as normal or was corrected took part in the study for payment. Written informed consent was obtained from all participants prior to the experiment, which was approved by the Biomedical Ethical Committee of the University of Louvain. The study conformed to the 2013 WMA Declaration of Helsinki.

Visual stimulation

Fifteen full-front color pictures of faces from a well-known database were used (The Max Planck Institute, Tübingen, Germany). To differentially tag the parts of a face, each face was vertically cut into two halves (Fig. 1A). Hence, a 'part', namely a subset of the whole face structure, is the entire half of a face in this paradigm. Each face half subtended a visual angle of approximately 6.04° in height and 4.3° in width. The face stimuli identities were unfamiliar to the participants. Stimuli were displayed on a light grey background (38 cd/m^2) using an in-house application (SinStim) written in MATLAB (MathWorks Inc., Natick, MA, USA). The design relied on the frequency-tagging EEG (or magnetoencephalograph) technique introduced by Regan & Heron (1969) (see, e.g. Appelbaum *et al.*, 2006; Müller *et al.*, 2006; Andersen *et al.*, 2009; Sutoyo & Srinivasan, 2009). In each trial of stimuli presentation, a face was divided into left and right halves flickering at different frequencies, for a duration of 70 s. The two half faces were sinusoidally contrast modulated, one at 5.88 Hz and the other at 7.14 Hz (Fig. 1B) (see also Boremanse *et al.*, 2013).

In the main condition ('Whole'), the two halves were arranged as a typical whole face [see Movie S1 for 'Different' identity repetition (Diff_ID_L7_R6_Whole.mov) and Movie S2 for 'Same' identity repetition (Same _ID_L7_R6_Whole.mov)]. Three control conditions were also tested. In the first control condition ('Gap'), the left and right face halves were separated by a 0.3° gap. In the second control condition ('Misaligned'), the face halves were spatially misaligned along the vertical axis (Fig. 1C) [see Movie S3 for 'Different' identity repetition (Diff_ID_L7_R6_Misaligned.mov) and Movie S4 for 'Same' identity repetition (Same _ID_L7_R6_ Misaligned.mov)]. The 'Gap' condition was designed to disrupt local interactions and was inspired by previous EEG frequency-tagging experiments investigating local interactions for low-level visual stimuli (Ratliff & Zemon, 1982; Zemon & Ratliff, 1982; Norcia *et al.*, 1999; Hou *et al.*, 2007; Appelbaum *et al.*, 2008). In this 'Gap' condition, although the gap was small and the face was still presented as a whole, the face was cut into two parts along its main axis [unlike the gap separating the top and bottom halves of a composite face, see Rossion (2013)]. This vertical cut created a disintegrated face stimulus, cutting in two all of the main diagnostic parts of a face (i.e. eyes/eyebrows region, mouth). Moreover, the observers were asked to fixate in between the two halves, i.e. outside the face stimulus. The vertical misalignment was performed in order to disrupt the integration of object parts while keeping the physical border between the two parts of equal length. Thus, in the second control condition, the face halves were also elongated (7° in height) so that they shared the same length of common border as in the 'Whole-face' condition. The width of the face was kept identical to the other two conditions in order to minimize any potential amplitude increase of the SSVEP due to an increase of stimulus size (Regan, 1989). This slight distortion of the stimulus was unnoticed by the participants, who were asked specifically about their impression of the elongated faces after the experiment. In the last control condition ('Inverted'), the stimuli were inverted in the picture plane. This manipulation is known to disrupt the perceptual integration of facial parts, to a larger extent for faces than for other visual stimuli (e.g. Yin, 1969; Young *et al.*, 1987; Tanaka & Farah, 1993; Biederman & Kalocsai, 1997; Rossion, 2008a).

Furthermore, there were two conditions of face identity presentation. In half of the trials, each participant was presented with a single face identity throughout the entire set of recordings (each of the 11 participants saw one out of 15 different faces). In the other half of the trials, the facial identity of each half face was randomly changed at each presentation, i.e. at the rate at which the face halves were contrast modulated ($f1$ and $f2$).

To summarize, participants were tested in eight different conditions – four position/orientation conditions of the face halves ('Whole-face', 'Gap', 'Misaligned' and 'Inverted') × two face identity conditions ('Same' and 'Different').

Procedure

After electrode-cap placement, participants were seated in a light- and sound-attenuated room at a viewing distance of 100 cm and performed each condition four times, for a total of 32 trials of 70 s each (38 min of experimentation in total). For half of the trials, the right side of the face (left visual field) was contrast modulated at 5.88 Hz and the left side (right visual field) at 7.14 Hz; for the remaining blocks, the modulation was reversed.

The design was controlled so that, in the first 16 trials, each participant performed the full set of conditions, counterbalanced for the side of the higher-frequency stimulation. The order of presentation of the 16 trials was randomized across participants. The next 16 trials were presented in reversed order for each participant, repeating the experiment. The total time of the experiment did not exceed 45 min (with pauses).

During each trial, participants were instructed to fixate a small black cross located in the centre of the face, below the eye line. They had to detect brief colour changes (200 ms, black to red) of the fixation cross (six to eight changes per trial) by pressing a response key. The goal of this task was to ensure that participants maintained a constant level of attention throughout the duration of the trials for all conditions. There were no differences between conditions in terms of hit rates and correct response times in this simple task (98% accuracy, mean response times of about 435 ms; no differences were found between orientation/position conditions or identity conditions). The triggers coding for each face half presentation were sent from the parallel port of the stimulation computer to the EEG recording computer at the beginning and end of the sequences, and at each minimal level of visual stimulation for each half face (the frame where only the uniform grey background was present, Fig. 1) (see also Rossion & Boremanse, 2011; Rossion *et al.*, 2012).

The choice of the specific stimulation frequencies, which were identical to our previous study (Boremanse *et al.*, 2013), was based on several factors. First, temporally close frequency rates were used because the SSVEP response characteristics depended on the temporal frequency of the visual input (Regan, 1989; Srinivasan *et al.*, 2006; Alonso-Prieto *et al.*, 2013). Second, the specific stimulation frequencies were constrained by the refresh rate of the monitor (i.e. integers of 100 Hz, 100/5.88 = 17; 100/7.14 = 14). Third, the fundamental frequencies of the evoked response, as well as at the second-order sum IM component (i.e. 5.88 + 7.14 = 13.02 Hz), were located outside the typical alpha frequency band [8–12 Hz, e.g. Klimesch (1999)], in order to maximize the signal-to-noise ratio (SNR) of these responses. Finally, stimulation frequencies between 4 and 9 Hz (theta band) appear to elicit maximal responses to contrast-modulated face stimulation as used here (Alonso-Prieto *et al.*, 2013).

Electroencephalographic recording

The electroencephalography was recorded using 128 Ag/AgCl electrodes placed on the scalp using a cap system (Waveguard128 cap, Cephalon A/S, Denmark). Electrode positions included the standard 10–20 system locations and additional intermediate sites (for a two-dimensional mapping of electrode labels and positions, see the 128-channel cap according to the five percent electrode system at http://www.ant-neuro.com/products/waveguard/electrode-layouts). The ground electrode was positioned on the forehead. Vertical and horizontal eye movements were monitored using four additional electrodes placed on the outer canthus of each eye and over the inferior and superior areas of the right orbit. During EEG recording, all electrodes were referenced to a centro-frontal channel (AFZ) and electrode impedances were kept below 10 kΩ. The electroencephalography was digitized at 1000 Hz (128 channel high-speed amplifier, Advanced Neuro Technology, The Netherlands) and a digital antialiasing filter of 0.27*sampling rate was applied at recording (at a sampling rate of 1000 Hz, the usable bandwidth was 0 to ~270 Hz).

Data analysis

The EEG analyses were carried out using Analyzer 2.0 (Brain Products, Germany), Letswave (http://nocions.webnode.com/letswave) (Mouraux & Iannetti, 2008), MATLAB and EEGLAB (http://sccn.ucsd.edu). Blocks of EEG recordings (12 blocks for each participant) were cropped to 66.67 s windows containing exactly 392 and 476 cycles of the two input frequencies $f1$ (5.88 Hz) and $f2$ (7.14 Hz), respectively. The first 2 s were removed to avoid contamination from transient responses triggered by the onset of visual stimulation train and to allow time for the system to be entrained by the stimulation (Rossion *et al.*, 2012). The EEG recording blocks were band-pass filtered between 0.1 and 100 Hz (Butterworth zero-phase filter, 24 db/oct) to remove slow drifts in the recorded signals and very high frequencies. The signals were then downsampled to 250 Hz in order to reduce the file size and increase the speed of data processing. Next, the segmented EEG recordings were averaged together for each condition and each participant separately (two blocks averaged by condition for each participant). Averaging in the time domain cancelled out EEG activity that was not phase-locked with the stimulus. The resulting average waveforms were then transformed into the frequency domain using a discrete Fastest Fourier Transform in the West, yielding an amplitude spectrum (μV) at values ranging from 0 to 100 Hz with a very high frequency resolution (1/66.67 = 0.015 Hz). For each electrode, SNR spectra were computed by taking the value at each frequency bin and dividing it by the average value of 20 neighbouring bins (Rossion & Boremanse, 2011). Finally, the spectra were averaged across participants for each condition separately, for the display of grand-averaged spectra and topographical maps. For statistical analysis (fundamentals and IM responses), the SNR values were averaged across channels of three regions of interest (ROIs), based on visual inspection of scalp topographies and on our previous studies with sinusoidal periodic contrast modulation (Rossion & Boremanse, 2011; Rossion *et al.*, 2012; Boremanse *et al.*, 2013). The ROIs included eight right occipito-temporal channels centred on channel PO8 (i.e. PO6, P8, PPO6h, P6, PO8, PPO10h, TPP8h and PO10), as well as the left homologous ROI centred on PO7 (i.e. PO5, P7, PO7, PPO5h, P5, PPO9h, TPP7h and PO9) and occipital medial channels around Oz (i.e. POO3h, POO4h, Oz, O1, O2, OI1h, OI2h and Iz).

Results

We first describe the results for the Whole-face condition, in which responses well above noise level were observed at the two fundamental stimulation frequencies, i.e. 5.88 and 7.14 Hz (Fig. 2; Table 1). There were responses until the fifth harmonic of each stimulation frequency (i.e. 29.40 and 35.70 Hz, respectively) but the largest responses were observed at the fundamental stimulation frequencies, with grand-averaged SNR values reaching 14.50 at 5.88 Hz and 14.76 at 7.14 Hz on medial-occipital channel Oz (i.e. 14.50× and 14.76× above the noise level, respectively). Mean (± SD) SNR values for each condition, each frequency of interest and each of the two visual field presentations are provided in Table 1 (see also the Tables S1–S3 in the Supporting Information for all SNR values with confidence intervals). All analyses were checked for sphericity violation (Mauchly's test) and corrected when necessary (Greenhouse–Geisser correction).

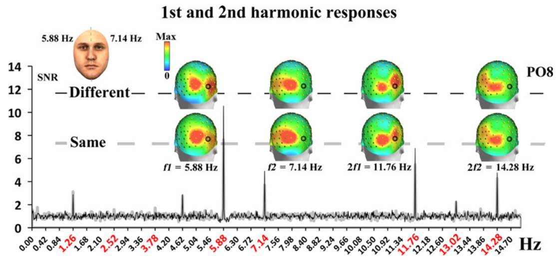

FIG. 2. Grand-averaged SNR spectrum (0–15 Hz) at right occipito-temporal channel PO8 (circled in black in the topographies) for the 'Whole-face' condition (left/right face halves stimulate the right/left visual field at 5.88 and 7.14 Hz) for the 'Different' (thin black line) and 'Same' (thick grey line) face-identity presentation topographic maps (above for 'Different', below for 'Same'). SNR spectra are computed by dividing each frequency bin (0.017 Hz) by the average of the 20 neighbouring bins. The colour scales of the topographical maps are different between conditions, ranging from 0 to the maximal SNR value of each condition (see Table 1). The IM components are indicated in red.

Part-based repetition suppression effects

Whole-face condition

We first describe part-based repetition suppression effects, i.e. responses at 5.88 and 7.14 Hz, for the 'Whole-face' condition. Maximal SNR values for 'Different' and 'Same' identity face conditions were located on the medial channel Oz, with larger responses following the stimulation of the left visual field than that of the right visual field (Fig. 2). Large responses were also found at occipito-temporal electrode sites contralateral to the side of stimulation. The largest responses were recorded on the same channels for both conditions, but the 'Different' condition exhibited significantly higher SNR values than the 'Same' condition (Table 1; Fig. 2).

For statistical comparisons, the channels included in each lateral ROI were pooled together and a repeated ANOVA was conducted with the factors *ROI* × *Visual field* × *Frequency* × *Identity* (3 × 2 × 2 × 2). A significant effect of *ROI* was found because the medial ROI showed larger responses than the lateral ROIs ($F_{2,20} = 4.50$, $P = 0.012$), which did not differ from each other ($F_{1,10} = 0.88$, $P = 0.185$). There was a significant effect of *Visual field* because the left visual field stimulation elicited higher responses than the right visual field stimulation ($F_{2,20} = 3.69$, $P = 0.042$). There was also a significant effect of *Identity* ('Different' > 'Same', $F_{2,20} = 44.13$, $P < 0.001$). A significant interaction between *ROI* and *Visual field* was also found, as expected (contralateral > ipsilateral response, $F_{2,20} = 8.81$, $P = 0.001$). There was also a significant interaction between *Frequency* and *Identity* ($F_{1,10} = 3.47$, $P = 0.046$) because the stimulation frequency at 5.88 Hz yielded a larger response than that at 7.14 Hz, but only for the 'Same' identity condition ($F_{1,10} = 10.19$, $P = 0.005$; NS for 'Different': $F_{1,10} = 0.9$, $P = 0.384$). These effects were qualified by a significant three-way interaction between *ROI*, *Visual field* and *Identity* ($F_{2,20} = 8.57$, $P = 0.001$). This interaction was due to larger repetition suppression effects at contralateral than ipsilateral sites [left visual field stimulation: right ROI (3.82) > central ROI (1.34) > left ROI (1.21); right visual field stimulation: left ROI (2.58) > central ROI (2.15) > right ROI (0.95)]. However, overall, considering both right and left visual field stimulations together, there was no difference in terms of the magnitude of the repetition suppression effect between ROIs (i.e. no two-way interaction between *ROI* and *Identity*, $P = 0.232$). An additional analysis

TABLE 1. Mean (± SD) SNR for the fundamental stimulation frequencies

		LVF stimulation						RVF stimulation					
		5.88 Hz			7.14 Hz			5.88 Hz			7.14 Hz		
		LH	Cent.	RH	LH	Cent.	RH	LH	Cent.	RH	LH	Cent.	RH
Whole	Different	4.89 (2.48)	10.24 (4.91)	10.71 (5.95)	4.55 (2.05)	10.41 (5.36)	9.87 (4.93)	8.99 (4.51)	8.89 (4.48)	4.25 (2.51)	8.11 (4.30)	9.20 (4.68)	4.85 (3.16)
	Same	4.13 (1.72)	8.77 (4.45)	7.43 (3.87)	2.89 (1.30)	8.77 (5.37)	5.50 (2.76)	6.65 (3.50)	7.14 (3.77)	3.79 (2.28)	5.27 (3.15)	6.40 (3.12)	3.42 (2.15)
Gap	Different	5.52 (2.38)	11.18 (4.31)	11.23 (7.11)	4.64 (2.16)	11.56 (5.65)	8.55 (4.85)	9.78 (5.14)	10.15 (5.82)	4.42 (2.40)	7.98 (4.36)	10.32 (5.26)	4.59 (3.08)
	Same	4.39 (2.19)	9.64 (5.14)	7.52 (4.60)	3.73 (1.38)	10.59 (5.46)	5.57 (2.38)	7.43 (4.57)	9.09 (4.38)	3.99 (2.44)	4.87 (3.11)	9.46 (4.40)	3.45 (2.05)
Mis.	Different	5.81 (2.90)	9.67 (5.30)	10.87 (6.34)	4.78 (2.36)	10.88 (5.86)	8.32 (5.15)	9.84 (5.99)	9.74 (5.81)	4.90 (2.46)	7.38 (5.59)	11.17 (5.95)	5.26 (3.08)
	Same	4.28 (2.30)	8.24 (4.46)	8.29 (4.85)	3.48 (1.75)	8.83 (5.26)	5.50 (2.78)	7.62 (4.89)	9.90 (5.76)	5.38 (3.30)	5.56 (3.57)	9.59 (5.53)	3.89 (2.57)
Inv.	Different	5.37 (2.33)	9.27 (5.03)	9.67 (5.96)	4.70 (2.10)	8.15 (4.49)	8.27 (5.33)	8.34 (5.00)	8.24 (4.97)	4.20 (2.19)	7.66 (4.28)	8.09 (3.50)	4.71 (2.64)
	Same	5.28 (2.61)	8.24 (5.34)	6.83 (4.45)	2.85 (1.65)	6.10 (3.85)	5.16 (3.63)	6.38 (3.90)	7.05 (4.53)	3.68 (1.96)	5.59 (2.70)	5.70 (3.77)	2.51 (1.22)

Mis., misaligned faces; Inv., inverted faces; LVF, left visual field; RVF, right visual field; Cent., center.

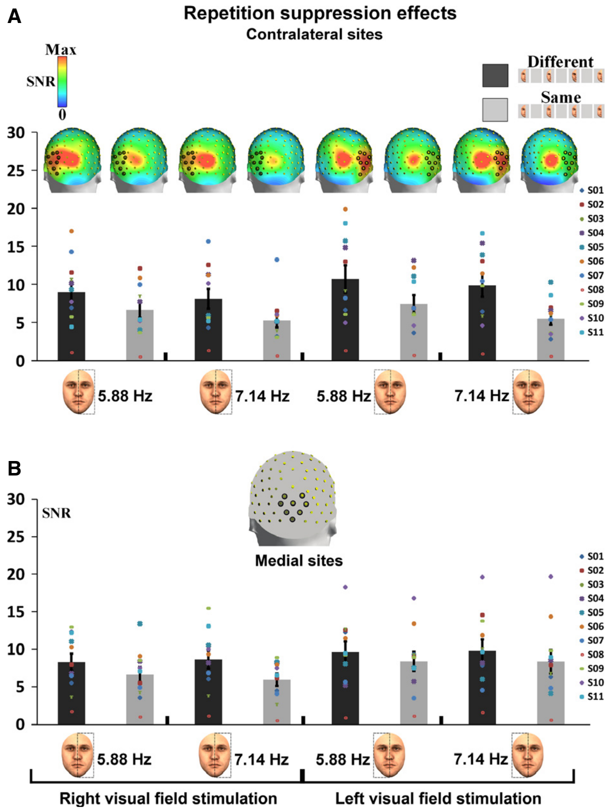

FIG. 3. (A) Above – topographic maps of the mean SNR for the left and right face half stimulation for the 'Whole-face' condition. Below – the bar graphs show the group mean (± SE) and individual values of the contralateral responses in SNR for the left and right visual field stimulation and for the 'Different' and 'Same' face-part presentation at the fundamental frequencies of stimulation (see Supporting Information Fig. S1 for bar graphs of differences). The channels used are: PO7, PO5, P7, PPO5h, P5, PPO9h, TPP7h and PO9, and PO8, PO6, P8, PPO6h, P6, PPO10h, TPP8h and PO10 for the LH and RH, respectively, marked in black in the topographies. (B) The bar graphs for the eight medial-occipital channels (OZ, POO3h, POO4h, O1, O2, OI1h, OI2h and Iz) of the medial ROI (marked in black on the topography above the histograms). Note that the face flicker eliciting the displayed response is outlined by a dashed line.

specifically investigating potential differences between the left and right hemispheres (LH and RH) in terms of the repetition suppression effect for contralateral stimulations (left visual field and right visual field for the right and left hemispheric ROIs, respectively) did not reveal any significant effect ($F_{1,10} = 2.15$, $P = 0.087$).

In summary, there were significant repetition suppression effects to the face parts (Fig. 3), more so for contralateral than ipsilateral stimulation (Table 1). However, importantly, these repetition suppression effects were found at all posterior sites, including occipital medial electrodes (Fig. 3B), with no difference between medial and lateral occipital ROIs.

Comparison of conditions

In order to compare repetition suppression effects across conditions, responses to 'Same' face-identity presentation were subtracted from responses to 'Different' face identity presentation for each of the four position/orientation conditions (i.e. 'Whole-face', 'Gap', 'Misaligned' and 'Inverted'). A repeated-measures ANOVA was then conducted with the factors *ROI* × *Visual field* × *Frequency* × *Condition* (3 × 2 × 2 × 4).

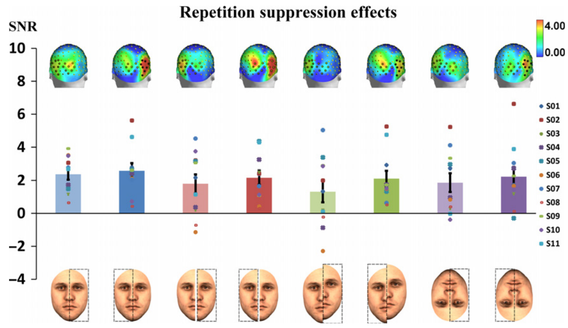

FIG. 4. Above – topographic maps of the mean differential ('different' – 'same') SNR for the left and right face half stimulation for the four conditions. Below – the bar graphs show the group means (± SE) and individual values for part-based face-identity repetition suppression effects of the medial and contralateral responses (collapsed together) in SNR for the left and right visual field stimulation at the fundamental frequency (*f1* and *f2* combined). The eight left and eight right lateral occipito-temporal channels were each combined with the eight medial-occipital channels (no difference in repetition suppression was found between the two lateral ROIs and medial ROI). The bar graphs depict the average of the channels that are marked in black on the topographies (above the bar graphs). The face flicker eliciting the displayed response is outlined by a dashed line.

The analysis showed a significant main effect of *Frequency*, the 7.14 Hz stimulation yielding larger repetition suppression effects than the 5.88 Hz stimulation ($F_{1,10} = 6.49$, $P = 0.015$). A significant interaction between *ROI* and *Visual field* was also found, reflecting the larger repetition suppression effect for contralateral over ipsilateral stimulation ($F_{2,20} = 11.66$, $P = 0.001$) (Table 1). Importantly, no other main effects or interactions were found; there were no differences between conditions in terms of the magnitude of the repetition suppression effect ($F_{3,30} = 1.27$, $P = 0.151$; Fig. 4; Table 1).

Intermodulation responses: difference components

*'Whole-face' condition: difference components (*nf2 − nf*1)*

Difference IM components (i.e. 1.26, 2.52, 3.78 and 5.04 Hz) emerged clearly above noise level on grand-averaged data for the repetition of the same identity in the 'Whole-face' condition (Fig. 5). These IM brain responses are unequivocally produced by neuronal populations that interact or integrate the two face parts nonlinearly (Zemon & Ratliff, 1984; Regan & Regan, 1988; Appelbaum *et al.*, 2008; Aissani *et al.*, 2011; Boremanse *et al.*, 2013). All of these IM components had a similar right occipito-temporal distribution (Fig. 5). However, for the 'Different' identity condition, only the first component at 1.26 Hz (also localized primarily over the right occipito-temporal cortex) was significantly above noise level (Fig. 5).

Only the lateral ROIs, where the IM components were found, were considered for statistical analysis. An ANOVA with the factors *Hemisphere* × *Identity* (2 × 2) was conducted, showing that the 1.26 Hz response did not differ between 'Same' and 'Different' identity presentations for the 'Whole-face' condition ($F_{1,10} = 0.65$, $P = 0.219$). The presence of the 1.26 Hz component indicated that left and right face parts were integrated even when the identity of each half was changed at each stimulation cycle. However, the absence of the other IM components indicated that the integration was reduced when face identity changed at every cycle compared with the repetition of the same identity.

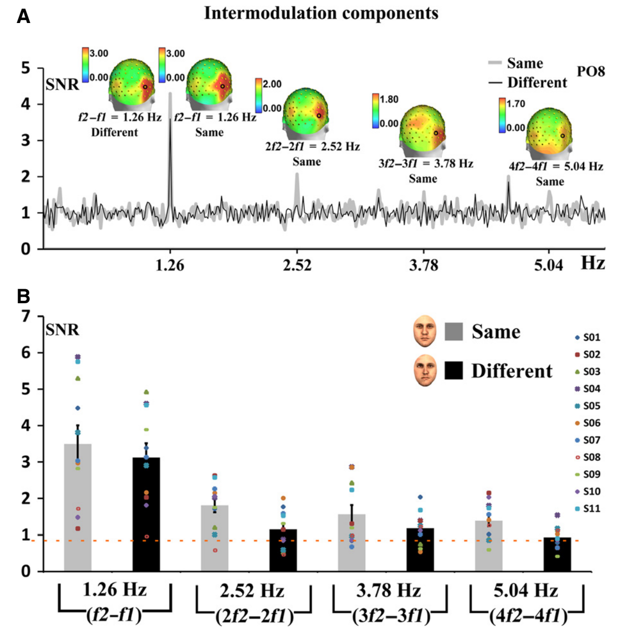

FIG. 5. (A) Grand-averaged SNR spectrum (0–5.6 Hz) at right occipito-temporal channel PO8 (circled in black in the topographies) for the ‘Whole-face’ condition, for the ‘Different’ (thin black line) and ‘Same’ (thick grey line) face-identity presentations (stimulation frequencies collapsed together). The component at 1.26 Hz with a right hemispheric advantage is present for both ‘Same’ and ‘Different’ face-identity presentations, whereas the other IM components are observed only for the ‘Same’ face stimulation. All IM components exhibit a similar right occipito-temporal topography. (B) SNR for the four IM components for ‘Same’ (grey) and ‘Different’ (black) face-identity presentation types. The bar graphs show the group mean (± SE) and SNR values for every individual tested of the eight right occipito-temporal channels (PO8, P8, PO6, P6, PPO6h, PPO10h, PO10 and TPP8h) selected in the right hemispheric ROI.

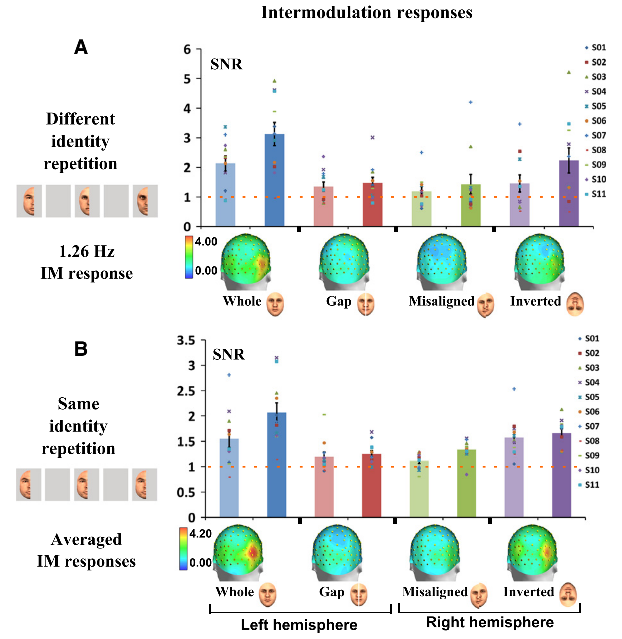

FIG. 6. (A) SNR averaged for the IM component at 1.26 Hz for ‘Different’ face-identity presentations and in B averaged for the difference IM components (i.e. at 1.26, 2.52, 3.78 and 5.04 Hz) for ‘Same’ face-identity presentation. Group means (± SE) and individual SNR values for the mean of the eight left and eight right occipito-temporal channels are shown. Topographic maps (back of the head) corresponding to the same conditions are depicted below each bar graph.

Main condition: difference components ($nf2 - mf1$)

Other difference IM components were found at 4.62 Hz ($1f2 - 2f1$) and 8.40 Hz ($1f1 - 2f2$), and these were present for both ‘Same’ and ‘Different’ identity presentations for the ‘Whole-face’ condition (Fig. 5A). An ANOVA with the factors *Hemisphere* × *Identity* (3 × 2) showed a main effect of *Hemisphere* for the 4.62 Hz component only, which was mainly localized in the right and medial ROIs ($F_{1,13} = 4.55$, $P = 0.046$; NS for 8.40 Hz: $F_{2,20} = 2.12$, $P = 0.146$). There was no main effect of *Identity* (4.62 Hz: $F_{1,10} = 0.002$, $P = 0.967$; 8.40 Hz: $F_{1,10} = 0.47$, $P = 0.504$) or interaction between the two factors (4.62 Hz: $F_{2,20} = 0.29$, $P = 0.752$; 8.40 Hz: $F_{2,20} = 0.27$, $P = 0.766$).

Comparison of conditions

Further analyses focused on the comparison between the ‘Whole-face’ condition and the three control conditions (i.e. ‘Gap’, ‘Misaligned’ and ‘Inverted’) for ‘Same’ and ‘Different’ face-identity presentations separately (data collapsed across visual fields and stimulation frequencies). The average of the four IM components present in the ‘Same’ condition was computed and all statistical analyses presented herein were carried out on these averaged values (see Boremanse *et al.*, 2013). For ‘Different’ presentations, only the component at 1.26 Hz was considered (neither the ‘Whole-face’ nor the control conditions showed further significant IM components). The channels included in each ROI were pooled together and a repeated ANOVA was conducted with the factors *Hemisphere* × *Condition* (2 × 4).

For ‘Same’ faces, IM components were virtually absent in the ‘Gap’ and ‘Misaligned’ conditions, replicating our previous observations (Boremanse *et al.*, 2013). Inverted faces led to substantial IM responses, which were nevertheless weaker than for upright faces in the RH only (Fig. 6). Statistical analyses confirmed these observations, showing a main effect of *Hemisphere* (Figs 7 and 8) (RH > LH, $F_{1,10} = 5.92$, $P = 0.017$), and a main effect of *Condition* ($F_{3,30} = 15.24$, $P < 0.001$). These effects were qualified by a two-way interaction between the factors *Hemisphere* and *Condition* ($F_{3,30} = 2.69$, $P = 0.032$) because the difference between the ‘Whole-face’ condition and other conditions was more prominent in the right than in the LH (‘Whole-face’ vs. control conditions: LH, $F_{1,10} = 3.43$, $P = 0.046$; RH, $F_{1,10} = 16.89$, $P = 0.001$). There was a significant difference between the ‘Whole-face’ and ‘Inverted’ conditions in the right ROI only ($F_{1,10} = 5.63$ $P = 0.019$; LH: $F_{1,10} = 0.07$, $P = 0.394$), whereas the comparison between ‘Whole-face’ and the other two control conditions was significant in both hemispheres (LH: P-values < 0.049; RH: P-values < 0.001).

For ‘Different’ faces, there were similar results, with a significant main effect of *Hemisphere*, the right ROI yielding the largest responses ($F_{1,10} = 3.32$, $P = 0.049$), and a significant main effect of *Condition* ($F_{3,30} = 15.77$, $P < 0.001$). Although the difference between the ‘Whole-face’ condition and the other conditions was larger in the RH, the interaction failed to reach significance ($F_{3,30} = 1.73$, $P = 0.090$) and the ‘Whole-face’ advantage over all control conditions was present in both hemispheres (LH: $F_{1,10} = 17.33$, $P < 0.001$; RH: $F_{1,10} = 29.49$, $P < 0.001$). There was a significant difference between the ‘Whole-face’ and ‘Inverted’ conditions in both ROIs (RH: $F_{1,10} = 27.61$ $P < 0.001$; LH:

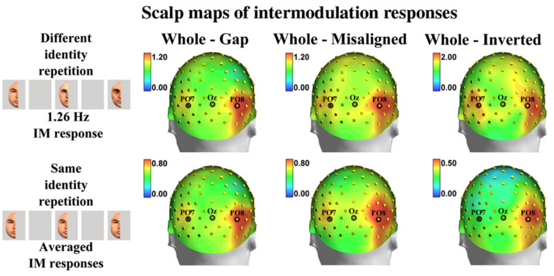

FIG. 7. Topographic maps (back of the head) of the SNR differences between the 'Whole-face' and control conditions showing that maximal differences are concentrated on the right occipito-temporal ROI and to a lesser extent on the left homologous region. 'Different' and 'Same' face-identity presentations are displayed above and below, respectively. The topographies for 'Different' show the distribution of the response at 1.26 Hz, which was the only difference IM response found in this condition. The topographies for 'Same' show the distribution of the mean of the four difference IM responses at 1.26, 2.52, 3.78 and 5.04 Hz.

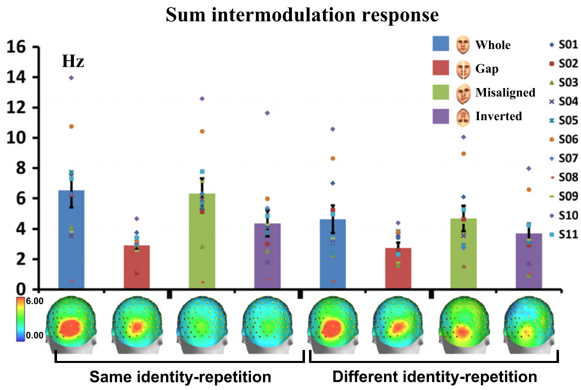

FIG. 8. Above – SNR for the sum IM component at 13.02 Hz in the four conditions of interest for 'Same' and 'Different' face-identity presentations, showing the group means (± SE) and SNR values for every individual tested for the mean of the eight channels selected for the medial ROI analysis. Below – the topographical maps (back of the head) relating to the bar graphs depicted above. All significant differences (all P-values < 0.05) between the four conditions of interest were found for both 'Same' and 'Different' face-identity presentations.

$F_{1,10} = 7.41$, $P < 0.01$; 'Whole-face' vs. each of the other conditions, P-values < 0.001).

For the IM responses at 4.62 and 8.40 Hz, the 'Whole-face' condition elicited significantly larger responses than the control conditions at 8.40 Hz only ('Same' identity: $F_{3,30} = 4.22$, $P = 0.007$; 'Different' identity: $F_{3,30} = 2.42$, $P = 0.042$; NS at 4.62 Hz: 'Same', $F_{3,30} = 0.20$, $P = 0.449$; 'Different' identity, $F_{3,30} = 1.63$, $P = 0.101$).

Intermodulation responses – sum component ($f1 + f2 = 13.02$ Hz)

Whole-face condition

As also observed previously, the sum component at 13.02 Hz was spread out over the temporal-occipital cortex for both 'Same' and 'Different' identity conditions, with maximal values on medial channel Oz (Fig. 8).

An ANOVA with the factors *Hemisphere* × *Identity* (3 × 2), for which the medial ROI was included, showed a main effect of *Hemisphere*, the responses for both identity repetitions being larger for the medial ROI than for the two lateral ROIs ($F_{1,12} = 10.74$, $P = 0.006$), whose responses did not differ from each other ($F_{1,10} = 0.59$, $P = 0.23$). Stimulating with the same facial identity elicited a higher response than stimulating with different facial identities (*Identity*, $F_{1,10} = 20.93$, $P < 0.001$). A significant interaction between *Hemisphere* and *Identity* ($F_{2,20} = 5.86$, $P = 0.005$) along with contrast analyses further revealed that this effect was only significant for the medial and left ROIs (left ROI: $F_{1,10} = 5.38$, $P = 0.042$; medial ROI: $t_{1,10} = 14.98$, $P = 0.003$; NS for the right ROI: $F_{1,10} = 0.41$, $P = 0.533$).

Comparison of conditions

For the $f1 + f2$ component, the 'Whole-face' condition was compared with the control conditions for each face identity condition separately. For the 'Same' identity presentation, a repeated ANOVA was conducted with the factors *Hemisphere* and *Condition* (3 × 4), which revealed a significant main effect of *Hemisphere* due to the medial ROI higher responses in all conditions ($F_{1,11} = 18.00$, $P < 0.001$) and a significant main effect of *Condition* ($F_{3,30} = 14.08$, $P < 0.001$) due to lower responses for the 'Gap' and 'Inverted' conditions than the 'Whole-face' and 'Misaligned' conditions (Fig. 8), which did not differ significantly from each other ($F_{1,10} = 1.58$, $P = 0.119$). The responses for the 'Inverted' condition were significantly larger than those for the 'Gap' condition ($F_{1,10} = 17.59$, $P < 0.001$). A significant interaction between *Hemisphere* and *Condition* showed that the 'Gap' condition systematically yielded lower responses than the other conditions at all ROIs ($F_{6,60} = 7.41$, $P < 0.001$), in contrast to the 'Inverted' condition, which only elicited a lower response than the 'Whole-face' and 'Misaligned' conditions at the medial ROI ($F_{2,20} = 11.87$, $P < 0.001$). Thus, the analysis revealed similar response trends for the 'Whole-face', 'Gap' and 'Misaligned' conditions across ROIs, i.e. larger responses in the medial ROI and no difference between the two lateral ROIs. However, for the 'Inverted' condition, the medial ROI responses were only larger compared with the left ROI ($F_{1,10} = 7.28$, $P = 0.022$), but not the right ROI ($F_{1,10} = 1.60$, $P = 0.234$).

The same analysis was carried out for the 'Different' identity presentation. Identical responses were found for the factor *Hemisphere* ($F_{1,12} = 5.53$, $P = 0.031$) and the factor *Condition* ($F_{3,30} = 6.63$, $P = 0.001$). However, the significant interaction between *Hemisphere* and *Condition* showed slightly different results ($F_{6,60} = 2.77$, $P = 0.01$). The four conditions yielded different responses in the medial ROI only ($F_{3,30} = 6.89$, $P < 0.001$; Fig. 8; NS for left and right ROIs: $F_{3,30} = 1.01$, $P = 0.201$ and $F_{3,30} = 0.50$, $P = 0.343$, respectively) where the 'Whole-face' and 'Misaligned' conditions, which did not differ from each other ($F_{1,10} = 0.06$, $P = 0.812$), showed higher responses than the 'Inverted' and 'Gap' conditions ($F_{1,10} = 9.22$, $P = 0.012$; 'Inverted' vs. 'Gap', NS: $F_{1,10} = 3.78$, $P = 0.080$).

Discussion

Part-based repetition suppression effects

Previous studies have shown release from repetition suppression/adaptation when only part of a face changes between repeated stimuli. For instance, changing the unattended bottom half of a face causes release from adaptation to the repetition of the same face in the functional magnetic resonance imaging signal obtained in face-selective areas of the right ventral occipito-temporal cortex (Schiltz & Rossion, 2006; Schiltz *et al.*, 2010). Similarly, there is a release from repetition suppression in the so-called fusiform face area

(Kanwisher *et al.*, 1997) to composite images in which either the internal or external parts change (Andrews *et al.*, 2010; Axelrod & Yovel, 2010), when either the eyes or mouth change (Harris & Aguirre, 2010) or the eyes and top face half change (Lai *et al.*, 2014). Event-related potential studies have also shown modulations of the N170 face-sensitive component (Bentin *et al.*, 1996) following changes of parts of a face (Jacques & Rossion, 2009). A fundamental limitation of these studies is that they cannot isolate the adaptation that is specific to the part from the adaptation of a combination of the parts, possibly the whole face. Indeed, changing one part changes the perception of the whole face stimulus (Sergent, 1984; Young *et al.*, 1987; Tanaka & Farah, 1993; Rossion, 2013). Consequently, these effects can be (and are often) interpreted in terms of holistic face processing, namely the processing/representation of the face as a single unit, with no high-level part structure (Tanaka & Farah, 1993; Rossion, 2008a, 2013). More generally, a large part such as half of a face, or even a small part such as the eye region alone, may be sufficient to trigger the representation of the whole face. Hence, putative repetition suppression effects obtained by repeating parts of faces cannot be interpreted as reflecting part-based repetition suppression effects.

Here, utilizing EEG frequency tagging, we were able to measure the adapted response to a part (i.e. a subset of the face, half of the face here) embedded in a whole face, and to objectively separate this response from a simultaneously recorded response to the other face part, as well as to an integrated representation between the two parts (IM components).

Large repetition suppression effects in response to face halves were found over posterior electrode sites, thus providing the first evidence of pure part-based face identity adaptation. Repetition suppression effects were largest on the hemisphere contralateral to the stimulation. Although there was an overall higher response in the RH than the LH, the contralateral part-based repetition suppression effect did not differ significantly between hemispheres, and was even relatively large at medial-occipital channels (around Oz; Fig. 3). This scalp topography is usually associated with low-level SSVEP responses (e.g. Müller *et al.*, 1998; Di Russo & Spinelli, 2002; Srinivasan *et al.*, 2006), even when complex visual stimuli such as faces are used (e.g. McTeague *et al.*, 2011). This observation is in contrast to the repetition suppression effects observed when the whole face changes identity at a periodic rate of 3–8 Hz, these effects being focused over the right occipito-temporal cortex, with no effect at medial-occipital electrode sites (Rossion & Boremanse, 2011; Rossion *et al.*, 2012). Although the spatial resolution of electroencephalography is inherently limited, this contrast suggests that part-based face identity repetition suppression effects, as reported here, are driven by low-level processes. Supporting this suggestion, whereas for whole faces a much larger repetition suppression effect is observed at 5.88 Hz than at 7.14 Hz (Alonso-Prieto *et al.*, 2013), here the stimulation frequency at 7.14 Hz yielded the largest part-based effects.

Most importantly for this point, part-based repetition suppression effects remained equally large whether the two parts formed a whole face or were horizontally separated, vertically misaligned, or inverted. Again, this observation contrasts with the large reduction of the repetition suppression effect that is observed for inverted whole faces (Rossion & Boremanse, 2011; Rossion *et al.*, 2012) and offers strong support for the view that these part-based effects, isolated here for the first time, are essentially low level.

Regarding this interpretation, there is only one caveat that we can think of. Here, contrary to our previous studies with whole faces flickering at a single frequency, the stimulus size did not change at each presentation cycle because the left and right halves of the face had to be identical in size in order to form a whole face. This absence of size variation may have increased low-level repetition suppression effects, possibly contributing to their wide distribution over all of the posterior electrodes. However, this factor cannot explain why the part-based effects remained equally strong when the face halves were separated, misaligned or inverted.

Intermodulation responses as evidence for high-level, holistic representation of faces

A face stimulus whose left and right halves are tagged at different frequencies elicited the same kind of IM responses as recently reported (Boremanse *et al.*, 2013). These responses emerge from nonlinear combinations of the part-evoked responses and are therefore found at differences and sums of the stimulation frequencies. They can only be generated by neuronal populations that receive information from both flickering stimuli (e.g. Regan & Regan, 1988; Appelbaum *et al.*, 2008; Giani *et al.*, 2012), here two face halves. This replication strengthens previous conclusions that the whole of a face is different to the sum of its parts (Boremanse *et al.*, 2013). Importantly, as in this previous study, the four difference terms (i.e. $f1–f2$ = 1.26 Hz; $2f1–2f2$ = 2.52 Hz, etc.) are found mainly over the right occipito-temporal cortex, suggesting that they are generated in high-level visual areas.

In the control condition when the two face halves are spatially separated ('Gap' condition), these difference IM components and the second-order sum ($f1 + f2$ = 13.02 Hz) IM response located on medial-occipital areas disappear. This observation is in line with the findings of our previous study, as well as with several EEG studies showing a reduction of occipital IM responses for spatially separated low-level visual stimuli (Zemon & Ratliff, 1982; Norcia *et al.*, 1999; Victor & Conte, 2000), or spatially separated stimuli outside fixation and moving away from each other (Fuchs *et al.*, 2008). A reduction of IM responses in lower-order and higher-order areas has also been observed when there is a texture-defined border between two flickering stimuli, such as a figure and background (Appelbaum *et al.*, 2008). The sum component (13.02 Hz) has a medial-occipital topography. Moreover, exactly as we observed previously (Boremanse *et al.*, 2013), it is still present in the 'Misaligned' condition, when there was no physical separation between the two parts and a contiguous border. This observation suggests that the sum component reflects local spatial interactions in early retinotopic areas that are more or less preserved by the misalignment manipulation. This may occur because there are still adjacent contrast regions across the border between the face parts that could interact in a fashion that does not depend on strict local or global alignment. By contrast, the multiple difference components (1.26 Hz, 2.52 Hz, etc.) over the right occipito-temporal cortex, the most interesting for our purpose, appear to depend on the global alignment of face parts in that the simple local juxtaposition of the parts is not sufficient to generate them.

The reduction of these IM difference responses in the control conditions clearly indicates that the IMs reflect high-level visual integration processes. Moreover, when faces are presented upside-down, the difference IM responses over the RH were selectively reduced. As the behavioural effects of inversion are observed exclusively for faces, or are much larger for faces than other object categories (Yin, 1969; Rossion, 2008a,b; for a review), this effect suggests that the IMs reflect at least partly face-specific neural responses. Importantly, this decrease of the IM responses for the three kinds of control conditions (i.e. Gap, Misalignment, Inversion) cannot be accounted for by the responses to face parts, which were unaffected by these manipulations. Thus, the neural response to an integrated face, as reflected in the IM responses, cannot be predicted by the magnitude of its responses to each of the face parts.

Most neurofunctional models of face and object perception consider that a visual stimulus is first decomposed part by part, and that these parts are only subsequently integrated into more global representations (Marr, 1982; Biederman, 1987; Jiang *et al.*, 2006; Ullman, 2007; DiCarlo & Cox, 2007). However, alternative models have been proposed according to which an initial coarse representation of the whole stimulus emerges in high-level visual areas, followed by a refinement of the visual representation involving lower-level visual areas through top-down processing (Mumford, 1992; Bullier, 2001; Hochstein & Ahissar, 2002; Rossion, 2008b; Rossion *et al.,* 2011). Our observations suggest that the representation of the parts of a face, when their measurement is isolated by frequency tagging, is low level; they are associated with a dominant topography over medial-occipital sites typical of low-level SSVEP responses, and they are unaffected by manipulations such as inversion. In contrast, the IM responses appear to be driven by high-level visual areas, in particular in the RH, sensitive to inversion. However, in the present frequency-tagging approach the phases of the IM components and of the fundamental responses cannot be directly compared, so that our data cannot be used to make direct inferences about the temporal hierarchy between the representation of the isolated parts and integrated parts.

In these first applications of the EEG frequency-tagging technique to facial parts (Boremanse *et al.*, 2013; the present study), we defined only two parts of a whole face – the left and right halves. The IMs might be generated only when a whole face stimulus is presented as a continuous surface, in the upright orientation. Alternatively, the IMs may be essentially generated by subregions of the face such as the eyes and eyebrows, and do not need the whole face stimulus to be present. Indeed, in the face perception literature, ‘holistic’ reflects a process by which a face stimulus is treated as an integrated unit (Rossion, 2008a). This process could be potentially applied to a subset of the face [i.e. a part; e.g. the eye/eyebrows region; see Rossion (2008a, 2013) for discussion of this issue]. For this reason, we cannot exclude that the same observations would be obtained by presenting only the eyes/eyebrows of a face for instance (i.e. comparing the eyes/eyebrows region at upright orientation vs. inverted, separated by a gap or misaligned) or even the mouth or nose alone. Future studies are now in a position to address this issue by frequency tagging subregions of the face (i.e. a mouth, an eye, etc.) in a systematic manner, for instance by using classification images or reverse correlation (Ahumada & Lovell, 1971) to faces (Haig, 1985) while measuring the EEG responses (Schyns *et al.*, 2007; Smith *et al.*, 2009).

A related issue concerns the reasons why the IMs virtually disappear in the Gap condition even though the stimulus is clearly perceived as a face. As noted by a reviewer of this article, such an apparently small manipulation (i.e. a gap of 0.3°) is unlikely to be associated with a large decrease of performance in a behavioural face recognition task for instance. Moreover, there is evidence of IM components between flickering stimuli that are presented outside fixation and separated by at least 0.25° (Fuchs *et al.*, 2008), so that this decrease of the IMs cannot be due to the size of the gap or the distance between fixation and the flickering face halves. However, in our stimulation paradigm, the fixation cross in the Gap condition falls exactly on the gap, i.e. outside the face stimulus. This suggests that, when stimuli are presented at frequency rates allowing only one fixation per face as here, fixating on the face stimulus may be critical (albeit not sufficient as indicated by the results of the misaligned and inverted face conditions) to integrate the two halves and thus elicit the IMs. Moreover, in the study of Fuchs *et al.* (2008), the IMs are present only if the figures are attended (by instruction), and not if the cross located outside the figures is attended. This raises the intriguing possibility that in the Gap condition of our study, attention to the face rather than the cross could elicit IM responses, meaning that selective attention to the face becomes necessary to integrate facial parts when they are separated by a gap. This possibility does not undermine our current results (where all conditions are tested with the same task and performance) but raises an interesting hypothesis to test in future studies.

Another issue worth exploring in future studies is whether the IM components would resist the introduction of a small gap that does not transform the main diagnostic internal parts of a face (i.e. the eyes and mouth) by breaking the stimulus along its main axis, as used here. For instance, a small gap between the top and bottom halves of a face, at the level of the nose or below the eyes, does not prevent human observers perceiving the stimulus as an integrated unit [i.e. the notorious composite face illusion, see Young *et al.* (1987), Hole (1994), and Rossion (2013) for a review]. Hence, it may be that a small gap between the top and bottom halves does not abolish the IMs, in particular if observers keep fixating on the nasion, typically the first fixation point on a face (Hsiao & Cottrell, 2008) and the optimal fixation point for an ideal observer using information across the whole face (Peterson & Eckstein, 2012).

A non-negligible advantage of the present EEG frequency-tagging approach with faces is that it leads to very high SNR responses (Regan, 1989; Rossion & Boremanse, 2011), allowing the measurement of the responses of interest in a few trials and including several control conditions in the paradigm. Also, the frequency-tagging approach used here is behaviour-free, requiring no explicit task to process the facial identity of either the whole face or face parts. Hence, the low attentional and task demands of this paradigm also make it well suited to work with difficult-to-test populations such as infants, young children or brain-damaged patients, especially as reliable responses can be obtained in individuals in just a few trials. However, for this very reason, we do acknowledge that we do not know at this stage how the part-based and integrated EEG responses relate to other neurofunctional and behavioural measurements of face recognition, and to interindividual face-processing abilities in general, in particular in holistic face perception (e.g. DeGutis *et al.*, 2013). In the same vein, another issue worth investigating in future studies is whether these EEG responses can be modulated by the behavioural task relevance of the parts or of the whole face.

Changing face identity interferes with visual integration of facial parts

As discussed above, changing the identity of the face parts at every cycle of stimulation substantially increased the magnitude of the part-based responses, an effect interpreted in terms of release from repetition suppression/adaptation. In contrast, varying the face part identities reduced the number and amplitude of several IM responses. This observation provides yet another double dissociation between part-based and holistic face responses. At first glance, the absence of release from adaptation for the IM responses may be puzzling because it contrasts with large release from repetition suppression when the whole face flickers at a single frequency (Rossion & Boremanse, 2011; Rossion *et al.*, 2012). However, changing the identity of each face half at a different frequency rate leads to whole faces that are made of different face halves, and second-order IM components can be negligible when the two inputs are markedly different [e.g. in contrast (Tsai *et al.*, 2012)]. Here, even though the different faces were carefully adjusted in order to form a continuous overall shape (i.e. they all had the same height), the width : height ratio of the face changed continuously during a stimulation sequence, making it more difficult to fit a holistic face template than when the same face identity is repeated. Moreover, the whole configuration of internal diagnostic parts (nose, mouth, combination of the eyes and eyebrows, etc.) is also disrupted to some extent when facial halves belonging to different identities are aligned with each other, possibly contributing to the reduction of the IM responses. All of these factors probably largely account for the lack of release from repetition suppression of the IM responses, to the point where opposite effects were observed here (i.e. larger IM responses for the repeated identity).

However, interestingly, for the 'Whole-face' condition, both of the identity conditions (i.e. 'Same' and 'Different') elicited the largest difference IM component at 1.26 Hz, whereas only the presentation of the same identity produced the three higher difference IM components at 2.52, 3.78 and 5.04 Hz. Likewise, whether or not the face parts varied in identity, only the first difference IM component at 1.26 Hz was found for inverted faces. These observations suggest that the different difference IM components reflect distinct visual integration processes. For now one can only speculate about the nature of these different integration processes. The process generating the lowest difference components appears to involve considerable temporal integration, as it only passes low-frequency interaction terms at its output. Hence, it could be that visual integration of facial parts is achieved more slowly when facial halves originate from different faces and change constantly. Likewise, the integration of facial parts may also be slowed down for inverted relative to upright faces, in agreement with the slower detection of faces when they are processed upside-down (e.g. Purcell & Stewart, 1988).

Conclusions

Separately frequency tagging the left and right halves of a face identified part-based repetition suppression effects on posterior electrode sites, these effects being unaffected when the two face halves were separated, misaligned, or inverted. In contrast, IM components were found essentially over the right occipito-temporal cortex and behave in the opposite direction, being significantly reduced following these manipulations. The IM components also decreased substantially for face halves belonging to different identities, which form a less coherent face than when they belong to the same face identity. These observations provide objective evidence for dissociation between part-based and integrated (i.e. holistic/configural) responses to faces in the human brain, showing not only that a whole face is different to the sum of its parts, but suggesting that only integrated responses may reflect high-level, face-specific representations.

Supporting Information

Additional supporting information can be found in the online version of this article:

Movie S1. Example of a stimulation sequence (7 s out of 70 s) in which the left half of the face flickers at 7.14 Hz and the right half at 5.88 Hz. Here, different face identities are presented at every stimulation cycle. Participants fixate the cross in the centre, just below the eyes of the face.

Movie S2. Example of a stimulation sequence (7 s out of 70 s) in which the left half of the face flickers at 7.14 Hz and the right half at 5.88 Hz. Here, the same face identity is presented at every stimulation cycle, as in Boremanse *et al.* (2013). Participants fixate the cross in the centre, just below the eyes of the face.

Movie S3. Example of a stimulation sequence (7 s out of 70 s) in which the left half of the face flickers at 7.14 Hz and the right half at 5.88 Hz, and the two halves are spatially misaligned from each other. Here, different face identities are presented at every stimulation cycle. Participants fixate the cross in the centre, just below the eyes of the face.

Movie S4. Example of a stimulation sequence (7 s out of 70 s) in which the left half of the face flickers at 7.14 Hz and the right half at 5.88 Hz, and the two halves are spatially misaligned from each other. Here, the same face identity is presented at every stimulation cycle. Participants fixate the cross in the centre, just below the eyes of the face.

Fig. S1. Complementary figure to Figure 3, showing the difference between the same and different face conditions (i.e. repetition suppression effects) for the whole face condition.

Table S1. Mean signal-to-noise ratios for the responses to the parts at the fundamental stimulation frequencies at 5.88 and 7.14 Hz (and ± 95% confidence intervals; L, M and R stand for left, medial and right ROI, respectively).

Table S2. Mean signal-to-noise ratios for the responses to the parts at the fundamental stimulation frequencies at 11.76 and 1.284 Hz (and ± 95% confidence intervals; L, M and R stand for left, medial and right ROI, respectively).

Table S3. Mean signal-to-noise ratios for integration responses for the mean of the three difference intermodulation responses (1.26, 2.52 and 3.78 Hz) and for the sum intermodulation response at 13.02 Hz (and ± 95% confidence intervals; only the values from the left and the right ROIs are represented).

Acknowledgements

This research was supported by an ERC grant (facessvep 284025). A.B. and B.R. are supported by the Belgian National Fund for Scientific Research (FNRS). The authors thank Talia Retter for her careful editing, as well as two anonymous reviewers for their helpful comments on a previous version of this article.

Abbreviations

EEG, electroencephalogram; IM, intermodulation; LH, left hemisphere; RH, right hemisphere; ROI, region of interest; SNR, signal-to-noise ratio; SSVEP, steady-state visual evoked potential.

References

Ahumada, A.J. Jr. & Lovell, J. (1971) Stimulus features in signal detection. *J. Acoust. Soc. Am.*, **49**, 1751–1756.

Aissani, C., Cottereau, B., Dumas, G., Paradis, A.L. & Lorenceau, J. (2011) Magnetoencephalographic signatures of visual form and motion binding. *Brain Res.*, **1408**, 27–40.

Alonso-Prieto, E., Belle, G.V., Liu-Shuang, J., Norcia, A.M. & Rossion, B. (2013) The 6 Hz fundamental stimulation frequency rate for individual face discrimination in the right occipito-temporal cortex. *Neuropsychologia*, **51**, 2863–2875.

Andersen, S.K., Müller, M.M. & Hillyard, S.A. (2009) Color-selective attention need not be mediated by spatial attention. *J. Vision*, **9**, 1–7.

Andrews, T.J., Davies-Thompson, J., Kingstone, A. & Young, A.W. (2010) Internal and external features of the face are represented holistically in face-selective regions of visual cortex. *J. Neurosci.*, **30**, 3544–3552.

Appelbaum, L.G., Wade, A.R., Vildavski, V.Y., Pettet, M.W. & Norcia, A.M. (2006) Cue-invariant networks for figure and background processing in human visual cortex. *J. Neurosci.*, **26**, 11695–11708.

Appelbaum, L., Wade, A., Pettet, M.W., Vildavski, V.Y. & Norcia, A.M. (2008) Figure–ground interaction in the human visual cortex. *J. Vision*, **8**, 1–19.

Axelrod, V. & Yovel, G. (2010) External facial features modify the representation of internal facial features in the fusiform face area. *NeuroImage*, **52**, 720–725.

Bentin, S., McCarthy, G., Perez, E., Allison, T. & Puce, A. (1996) Electrophysiological studies of face perception in humans. *J. Cognitive Neurosci.*, **8**, 551–565.

Biederman, I. (1987) Recognition-by-components: a theory of human image understanding. *Psychol. Rev.*, **94**, 115–147.

Biederman, I. & Kalocsai, P. (1997) Neurocomputational bases of object and face recognition. *Philos. T. Roy. Soc. B.*, **352**, 1203–1219.

Boremanse, A., Norcia, A.M. & Rossion, B. (2013) An objective neural signature for visual binding of face parts in the human brain. *J. Vision*, **13**, 1–18.

Bullier, J. (2001) Integrated model of visual processing. *Brain Res. Rev.*, **36**, 96–107.

DeGutis, J., Wilmer, J., Mercado, R.J. & Cohan, S. (2013) Using regression to measure holistic face processing reveals a strong link with face recognition ability. *Cognition*, **126**, 87–100.

Di Russo, F. & Spinelli, D. (2002) Effects of sustained, voluntary attention on amplitude and latency of steady-state visual evoked potential: a costs and benefits analysis. *Clin. Neurophysiol.*, **113**, 1771–1777.

DiCarlo, J.J. & Cox, D.D. (2007) Untangling invariant object recognition. *Trends Cogn. Sci.*, **11**, 333–341.

Fuchs, S., Andersen, S.K., Gruber, T. & Müller, M.M. (2008) Attentional bias of competitive interactions in neuronal networks of early visual processing in the human brain. *NeuroImage*, **41**, 1086–1101.

Giani, A.S., Ortiz, E., Belardinelli, P., Kleiner, M., Preissl, H. & Noppeney, U. (2012) Steady-state responses in MEG demonstrate information integration within but not across the auditory and visual senses. *NeuroImage*, **60**, 1478–1489.

Grill-Spector, K., Henson, R. & Martin, A. (2006) Repetition and the brain: neural models of stimulus-specific effects. *Trends Cogn. Sci.*, **10**, 14–23.

Haig, N.D. (1985) How faces differ – a new comparative technique. *Perception*, **14**, 601–615.

Harris, A. & Aguirre, G.K. (2010) Neural tuning for face wholes and parts in human fusiform gyrus revealed by FMRI adaptation. *J. Neurophysiol.*, **104**, 336–345.

Hochstein, S. & Ahissar, M. (2002) View from the top: hierarchies and reverse hierarchies review. *Neuron*, **36**, 791–804.

Hole, G.J. (1994) Configurational factors in the perception of unfamiliar faces. *Perception*, **23**, 65–74.

Hou, C., Good, W.V. & Norcia, A.M. (2007) Validation study of VEP vernier acuity in normal-vision and amblyopic adults. *Invest. Ophth. Vis. Sci.*, **48**, 4070–4078.

Hsiao, J.H. & Cottrell, G. (2008) Two fixations suffice in face recognition. *Psychol. Sci.*, **19**, 998–1006.

Jacques, C. & Rossion, B. (2009) The initial representation of individual faces in the right occipito-temporal cortex is holistic: electrophysiological evidence from the composite face illusion. *J. Vision*, **9**, 1–16.

Jiang, X., Rosen, E., Zeffiro, T., Vanmeter, J., Blanz, V. & Riesenhuber, M. (2006) Evaluation of a shape-based model of human face discrimination using FMRI and behavioral techniques. *Neuron*, **50**, 159–172.

Kanwisher, N., McDermott, J. & Chun, M.M. (1997) The fusiform face area: a module in human extrastriate cortex specialized for face perception. *J. Neurosci.*, **17**, 4302–4311.

Klimesch, W. (1999) EEG alpha and theta oscillations reflect cognitive and memory performance: a review and analysis. *Brain Res. Rev.*, **29**, 169–195.

Lai, J., Pancaroglu, R., Oruc, I., Barton, J.J. & Davies-Thompson, J. (2014) Neuroanatomic correlates of the feature-salience hierarchy in face processing: an fMRI-adaptation study. *Neuropsychologia*, **53**, 274–283.

Logothetis, N.K. & Sheinberg, D.L. (1996) Visual object recognition. *Annu. Rev. Neurosci.*, **19**, 577–621.

Marr, D. (1982) *Vision: A Computational Investigation into the Human Representation and Processing of Visual Information*, Phenomenology and the Cognitive Sciences. Freeman, New York.

Maurer, D., Grand, R.L. & Mondloch, C.J. (2002) The many faces of configural processing. *Trends Cogn. Sci.*, **6**, 255–260.

McTeague, L.M., Shumen, J.R., Wieser, M.J., Lang, P.J. & Keil, A. (2011) Social vision: sustained perceptual enhancement of affective facial cues in social anxiety. *NeuroImage*, **54**, 1615–1624.

Miller, E., Li, L. & Desimone, R. (1991) A neural mechanism for working and recognition memory in inferior temporal cortex. *Science*, **254**, 1377–1379.

Mouraux, A. & Iannetti, G.D. (2008) Across-trial averaging of event-related EEG responses and beyond. *Magn. Reson. Imaging*, **26**, 1041–1054.

Müller, M.M., Teder-Sälejärvi, W. & Hillyard, S.A. (1998) The time course of cortical facilitation during cued shifts of spatial attention. *Nat. Neurosci.*, **1**, 631–634.

Müller, M.M., Andersen, S., Trujillo, N.J., Valdés-Sosa, P., Malinowski, P. & Hillyard, S.A. (2006) Feature-selective attention enhances color signals in early visual areas of the human brain. *Proc. Natl. Acad. Sci. USA*, **103**, 14250–14254.

Mumford, D. (1992) On the computational architecture of the neocortex. II. The role of cortico-cortical loops. *Cybernetics*, **251**, 241–251.

Norcia, A.M., Wesemann, W. & Manny, R.E. (1999) Electrophysiological correlates of vernier and relative motion mechanisms in human visual cortex. *Visual Neurosci.*, **16**, 1123–1131.

Peterson, M.F. & Eckstein, M.P. (2012) Looking just below the eyes is optimal across face recognition tasks. *Proc. Natl. Acad. Sci. USA*, **109**, E3314–E3323.

Purcell, D. & Stewart, A. (1988) The face-detection effect: configuration enhances detection. *Percept. Psychophys.*, **43**, 355–366.

Ratliff, F. & Zemon, V. (1982) Some new methods for the analysis of lateral interactions that influence the visual evoked potential. *Ann. NY Acad. Sci.*, **388**, 113–124.

Regan, D. (1966) Some characteristics of average steady-state and transient responses evoked by modulated light. *Electroen. Clin. Neuro.*, **20**, 238–248.

Regan, D. (1989) *Human Brain Electrophysiology: Evoked Potentials and Evoked Magnetic Fields in Science and Medicine*. Elsevier, New York.

Regan, D. & Heron, J.R. (1969) Clinical investigation of lesions of the visual pathway: a new objective technique. *J. Neurol. Neurosur. Ps.*, **32**, 479–483.

Regan, M.P. & Regan, D. (1988) A frequency domain technique for characterizing nonlinearities in biological systems. *J. Theor. Biol.*, **133**, 293–317.

Ringo, J. (1996) Stimulus specific adaptation in inferior temporal and medial temporal cortex of the monkey. *Behav. Brain Res.*, **76**, 101–107.

Rossion, B. (2008a) Picture-plane inversion leads to qualitative changes of face perception. *Acta Psychol.*, **128**, 274–289.

Rossion, B. (2008b) Constraining the cortical face network by neuroimaging studies of acquired prosopagnosia. *NeuroImage*, **40**, 423–426.

Rossion, B. (2013) The composite face illusion: a whole window into our understanding of holistic face perception. *Vis. Cogn.*, **21**, 139–253.

Rossion, B. (2014) Understanding individual face discrimination by means of fast periodic visual stimulation. *Exp. Brain Res.*, **232**, 1599–1621.

Rossion, B. & Boremanse, A. (2011) Robust sensitivity to facial identity in the right human occipito-temporal cortex as revealed by steady-state visual-evoked potentials. *J. Vision*, **11**, 1–21.

Rossion, B., Dricot, L., Goebel, R. & Busigny, T. (2011) Holistic face categorization in higher order visual areas of the normal and prosopagnosic brain: toward a non-hierarchical view of face perception. *Front. Hum. Neurosci.*, **4**, 225.

Rossion, B., Prieto, E.A., Boremanse, A., Kuefner, D. & Van Belle, G. (2012) A steady-state visual evoked potential approach to individual face perception: effect of inversion, contrast-reversal and temporal dynamics. *NeuroImage*, **63**, 1585–1600.

Schiltz, C. & Rossion, B. (2006) Faces are represented holistically in the human occipito-temporal cortex. *NeuroImage*, **32**, 1385–1394.

Schiltz, C., Dricot, L., Goebel, R. & Rossion, B. (2010) Holistic perception of individual faces in the right middle fusiform gyrus as evidenced by the composite face illusion. *J. Vision*, **10**, 1–16.

Schyns, P.G., Petro, L.S. & Smith, M.L. (2007) Dynamics of visual information integration in the brain for categorizing facial expressions. *Curr. Biol.*, **17**, 1580–1585.

Sergent, J. (1984) An investigation into component and configural processes underlying face perception. *Brit. J. Psychol.*, **75**, 225–242.

Smith, M.L., Fries, P., Gosselin, F., Goebel, R. & Schyns, P.G (2009) Inverse mapping the neuronal substrates of face categorizations. *Cereb. Cortex*, **19**, 2428–2438.

Srinivasan, R., Bibi, F.A. & Nunez, P.L. (2006) Steady-state visual evoked potentials: distributed local sources and wave-like dynamics are sensitive to flicker frequency. *Brain Topogr.*, **18**, 167–187.

Sutoyo, D. & Srinivasan, R. (2009) Nonlinear SSVEP responses are sensitive to the perceptual binding of visual hemifields during conventional “eye” rivalry and interocular “percept” rivalry. *Brain Res.*, **1251**, 245–255.

Tanaka, J. & Farah, M. (1993) Parts and wholes in face recognition. *Q. J. Exp. Psychol.*, **46**, 225–245.

Thorpe, S., Fize, D. & Marlot, C. (1996) Speed of processing in the human visual system. *Nature*, **381**, 520–522.

Tsai, J., Wade, A. & Norcia, A. (2012) Dynamics of normalization underlying masking in human visual cortex. *J. Neurosci.*, **32**, 2783–2789.

Ullman, S. (2007) Object recognition and segmentation by a fragment-based hierarchy. *Trends Cogn. Sci.*, **11**, 58–64.

Victor, J.D. & Conte, M.M. (2000) Two-frequency analysis of interactions elicited by Vernier stimuli. *Visual Neurosci.*, **17**, 959–973.

Yin, R. (1969) Looking at upside-down faces. *J. Exp. Psychol.*, **81**, 141–151.

Young, A., Hellawell, D. & Hay, D. (1987) Configurational information in face perception. *Perception*, **16**, 747–759.

Zemon, V. & Ratliff, F. (1982) Visual evoked potentials: evidence for lateral interactions. *Proc. Natl. Acad. Sci. USA*, **79**, 5723–5726.

Zemon, V. & Ratliff, F. (1984) Intermodulation components of the visual evoked potential: responses to lateral and superimposed stimuli. *Biol. Cybern.*, **50**, 401–408.